

1 **Variability and Trends in Physical and Biogeochemical**  
2 **Parameters of the Mediterranean Sea during a Cruise with**  
3 **RV MARIA S. MERIAN in March 2018**

4  
5 **Dagmar Hainbucher<sup>1</sup>, Marta Álvarez<sup>4</sup>, Blanca Astray Uceda<sup>4</sup>, Giancarlo Bachi<sup>5</sup>,**  
6 **Vanessa Cardin<sup>3</sup>, Paolo Celentano<sup>6</sup>, Spyros Chaikakis<sup>7</sup>, Maria del Mar Chaves**  
7 **Montero<sup>3,9</sup>, Giuseppe Civitarese<sup>3</sup>, Noelia M. Fajar <sup>4</sup>, Francois Fripiat<sup>10</sup>, Lennart**  
8 **Gerke<sup>2</sup>, Alexandra Gogou<sup>7</sup>, Elisa Fernández Guallart<sup>4</sup>, Birte Gülk<sup>1</sup>, Abed El**  
9 **Rahman Hassoun<sup>8</sup>, Nico Lange<sup>2</sup>, Andrea Rochner<sup>1</sup>, Chiara Santinelli<sup>5</sup>, Tobias**  
10 **Steinhoff<sup>2</sup>, Toste Tanhua<sup>2</sup>, Lidia Urbini<sup>3</sup>, Dimitrios Velaoras<sup>7</sup>, Fabian Wolf<sup>2</sup>,**  
11 **Andreas Welsch<sup>1</sup>**

12 [1]{Institut für Meereskunde, CEN, Universität Hamburg, Bundesstraße 53, 20146 Hamburg,  
13 Germany}

14 [2]{GEOMAR, Helmholtz-Zentrum für Ozeanforschung Kiel, Wischhofstr. 1-3, 24148 Kiel,  
15 Germany}

16 [3]{Istituto Nazionale di Oceanografia e di Geofisica Sperimentale – OGS, Dept. Of  
17 Oceanography, Borgo Grotta Gigante 42/c, 34010 Sgonico, Trieste, Italy}

18 [4]{Instituto Español de Oceanografía (IEO), centro de A Coruña, Spain}

19 [5]{Istituto di Biofisica, CNR, Pisa, Italy}

20 [6]{Istituto di Scienze Marine, Venezia, Italy}

21 [7]{Hellenic Centre for Marine Research, Athens, Greek}

22 [8]{National Council for Scientific Research in Lebanon. National Center for Marine Sciences}

23 [9]{Centro Euro-Mediterraneo sui Cambiamenti Climatici CMCC, Bologna, Italy}

24 [10]{Max Planck Institute for Chemistry, Mainz, Germany}

25 *Correspondence to:* Dagmar Hainbucher (dagmar.hainbucher@uni-hamburg.de)

26

27

1 **Abstract**

2 The last decades have seen dramatic changes in the hydrography and biogeochemistry of the  
3 Mediterranean Sea. The complex bathymetry, highly variable spatial and temporal scales of  
4 atmospheric forcing, convective and ventilation processes contribute to generate complex and  
5 unsteady circulation patterns and significant variability in biogeochemical systems. Part of the  
6 variability of this system can be influenced by anthropogenic contributions. Consequently, it is  
7 necessary to document details and to understand trends in place to better relate the observed  
8 processes and to possibly predict the consequences of these changes. In this context we report  
9 data from an oceanographic cruise in the Mediterranean Sea on the German research vessel  
10 MARIA S. MERIAN (MSM72) in March 2018. The main objective of the cruise was to  
11 contribute to the understanding of long-term changes and trends in physical and biogeochemical  
12 parameters, such as the anthropogenic carbon uptake and to further assess the hydrographical  
13 situation after the major climatological shifts in the eastern and western part of the basin, known  
14 as the Eastern and Western Mediterranean Transients. During the cruise, multidisciplinary  
15 measurements were conducted on a predominantly zonal section throughout the Mediterranean  
16 Sea, contributing to the global GO-SHIP repeat hydrography program, and particularly to its  
17 Mediterranean Sea component, Med-SHIP, and adhering to the GO-SHIP requirements.

18  
19 **Data coverage and parameter measured**

20 Repository-Reference (table 1a and table 1b):

21

22

- 1 Table 1a. List of physical parameters from MARIA S. MERIAN cruise MSM72 as seen in the  
 2 PANGAEA database. PI: Dagmar Hainbucher

Parameter Name	Short name	Unit	Method	Comments
<b>DATE/TIME</b>	Date/Time			Geocode
<b>LATITUDE</b>	Latitude			Geocode
<b>LONGITUDE</b>	Longitude			Geocode
<b>Pressure, water</b>	Press	dbar	CTD, SEA_BIRD SBE 911plus	
<b>Temperature, water</b>	Temp	°C	CTD, SEA_BIRD SBE 911plus	
<b>Salinity</b>	Sal		CTD, SEA_BIRD SBE 911plus	PSU
<b>Oxygen</b>	O2	µmol/kg	CTD with attached oxygen sensor (SBE43) calibrated, corrected using Winkler titration	
<b>Pressure, water</b>	Press	dbar	Underway CTD (UCTD), Oceanscience	
<b>Temperature, water</b>	Temp	°C	Underway CTD (UCTD), Oceanscience	
<b>Salinity</b>	Sal		Underway CTD (UCTD), Oceanscience	PSU
<b>DEPTH, water</b>	Depth	m		
<b>Current velocity east-west</b>	UC	m/s	Shipboard Acoustic Doppler Current Profiling (SADCP)	
<b>Current velocity north-south</b>	VC	m/s	Shipboard Acoustic Doppler Current Profiling (SADCP)	
<b>DEPTH, water</b>	Depth	m		
<b>Current velocity east-west</b>	UC	m/s	lowered Acoustic Doppler Current Profiling (LADCP)	
<b>Current velocity north-south</b>	VC	m/s	lowered Acoustic Doppler Current Profiling (LADCP)	

3

4

- 1 Table 1b. List of biogeochemical parameters from MARIA S. MERIAN cruise MSM72 as
- 2 seen in the CCHDO database. PI: Toste Tanhua

Variable	Unit
Dissolved Oxygen (O <sub>2</sub> )	μmol kg <sup>-1</sup>
Sulphurhexafluorid (SF <sub>6</sub> )	fmol kg <sup>-1</sup>
CCl <sub>2</sub> F <sub>2</sub> (CFC-12)	pmol kg <sup>-1</sup>
Nitrate (NO <sub>3</sub> <sup>-</sup> )	μmol kg <sup>-1</sup>
Nitrite (NO <sub>2</sub> <sup>-</sup> )	μmol kg <sup>-1</sup>
Phosphate (PO <sub>4</sub> <sup>2-</sup> )	μmol kg <sup>-1</sup>
Silicate (Si)	μmol kg <sup>-1</sup>
Dissolved Inorganic Carbon (DIC)	μmol kg <sup>-1</sup>
Total Alkalinity (TA)	μmol kg <sup>-1</sup>
pH	Total scale @ 25°C
Carbonate (CO <sub>3</sub> <sup>2-</sup> )	μmol kg <sup>-1</sup>
δ <sup>13</sup> C of DIC	Per mille
Total Dissolved Nitrogen (TDN)	μmol kg <sup>-1</sup>
Total Dissolve Phosphorus (TDP)	μmol kg <sup>-1</sup>
CHClF <sub>2</sub> (HCFC-22)	pmol kg <sup>-1</sup>
C <sub>2</sub> H <sub>3</sub> Cl <sub>2</sub> F (HCFC-141b)	pmol kg <sup>-1</sup>
C <sub>2</sub> H <sub>3</sub> ClF <sub>2</sub> (HCFC-142b)	pmol kg <sup>-1</sup>
CH <sub>2</sub> FCF <sub>3</sub> (HFC-134a)	pmol kg <sup>-1</sup>
C <sub>2</sub> HF <sub>5</sub> (HFC-125)	pmol kg <sup>-1</sup>
CHF <sub>3</sub> (HFC-23)	pmol kg <sup>-1</sup>

3

4

- 1 <https://doi.pangaea.de/10.1594/PANGAEA.905902> (for CTD)  
2 <https://doi.pangaea.de/10.1594/PANGAEA.913512> (for UCTD)  
3 <https://doi.pangaea.de/10.1594/PANGAEA.913608> (for ADCP)  
4 <https://doi.pangaea.de/10.1594/PANGAEA.913505> (for IADCP)  
5 <https://doi.pangaea.de/10.1594/PANGAEA.905887> (for chemical data)  
6 <https://doi.org/10.25921/z7en-hn85> (for pCO<sub>2</sub>)

7 A link to the summary page of the cruise MSM72 can be found in the PANGAEA data base  
8 under: <https://www.pangaea.de/?q=msm72&f.campaign%5B%5D=MSM72>

9 Coverage: 34°N-41°N, 6°W-28°E

10 Location Name: The Mediterranean Sea

11 Date/Time Start: 2. March 2018

12 Date/Time End: 3. April 2018

13

## 14 **1. Introduction**

15 Contrary to earlier ideas that the Mediterranean Sea is always in a steady state, we now know  
16 in the light of new research that the Mediterranean Sea is not and it is potentially sensitive to  
17 climatic changes (Malanotte-Rizzoli, 2014). Proof of this are the drastic changes that the eastern  
18 Mediterranean (EMed) has undergone in the past. The largest climatic event, named Eastern  
19 Mediterranean Transient (EMT), occurred in the EMed between the late 1980's and early  
20 1990's, where deep-water formation switched from the Adriatic to the Aegean Sea. This  
21 episode modified the thermohaline characteristics of the outflow through the Sicily Channel,  
22 advecting anomalously salty and warm Levantine Intermediate Water (LIW) to the western  
23 Mediterranean Sea (WMed) and leading to a significant increase in temperature and salt in the  
24 intermediate and deep layers of the WMed. Additionally, strong deep convection induced by  
25 extreme atmospheric events during winter time 2004-2006 (low precipitation, cold, persistent  
26 winds) was also enhancing salt and temperature in the entire basin up to about 1600 m  
27 (Schroeder et al., 2006, Schroeder et al., 2008). This abrupt climate shift is referred to as  
28 Western Mediterranean Transient (WMT) and the physical changes are comparable to the EMT,  
29 both in terms of intensity and observed effects (Schroeder et al., 2008). The existence of both  
30 transients contradicts the hypothesis of a steady state. On the other hand, it has also been proven  
31 that an EMT has never been observed before (Roether et al., 2013).

1 The characteristic of the Mediterranean Sea is also such that it has the potential to sequester  
2 large amounts of anthropogenic CO<sub>2</sub>, Cant, since the Mediterranean Sea has high alkalinity and  
3 temperature, which can be rapidly transported to deep by the overturning circulation (e.g.  
4 Schneider et al., 2010). The column inventories of Cant in the Mediterranean are among the  
5 highest found in the world oceans; the Mediterranean Sea thus stores a significant portion of  
6 the global anthropogenic emissions of Cant despite its relatively small volume.

7 Furthermore, marine dissolved organic carbon (DOC) represents the largest reservoir of  
8 reduced carbon ( $662 \cdot 10^{15}$  g C) on Earth (Hansell, 2009), it therefore plays a major role in the  
9 global carbon cycle. Its role in the functioning of marine ecosystems is equally crucial since  
10 DOC is released at all the levels of the food web, as a byproduct of many trophic interactions  
11 and/or metabolic processes and is the main source of energy for the heterotrophic prokaryotes  
12 (Carlson and Hansell, 2015). Although most of DOC is produced in-situ, external sources  
13 (atmosphere, rivers, sediments) may affect its concentration and distribution. Physical  
14 processes, such as deep-water formation, thermohaline circulation, vertical stratification and  
15 mesoscale activities have been reported to be the main drivers of DOC distribution in the  
16 Mediterranean Sea (Santinelli, 2015, Santinelli et al., 2015, Santinelli et al., 2013, Santinelli,  
17 2010).

18 The main scientific objective of the cruise reported here was to add knowledge to the different  
19 scales and magnitudes of variability and trends in circulation, hydrography, and  
20 biogeochemistry of the Mediterranean Sea. Key variables were measured in strategic regions  
21 in order to understand changes, the reason for occurrence, and the drivers. In this context, this  
22 cruise is part of the Med-SHIP and GO-SHIP long-term repeat cruise section that is conducted  
23 at regular intervals in the Mediterranean Sea to observe changes and impacts on physical and  
24 biogeochemical variables.

25 The following science questions were addressed:

- 26 1. What are the long-term changes and/or trends in physics and biochemistry in the  
27 Mediterranean Sea, including all the sub-basins?
- 28 2. How is the hydrographic situation in the Mediterranean developing further after the EMT  
29 and WMT? Is there still a tendency of the system to return to the pre-EMT situation and is there  
30 a similar trend in the WMed?
- 31 3. How are eddies distributed in the EMed and WMed during the cruise? Do they differ in  
32 the sub basins? To what extent is heat and salt transferred into the vertical by eddies in the

1 WMed and EMed during the cruise period?

2 4. What is the uptake rate of the anthropogenic carbon in the Mediterranean and is this  
3 changing over time?

4 5. What is the extent of the variability and trends in the inventory of biogeochemical  
5 variables (including oxygen, nutrients and dissolved organic carbon)?

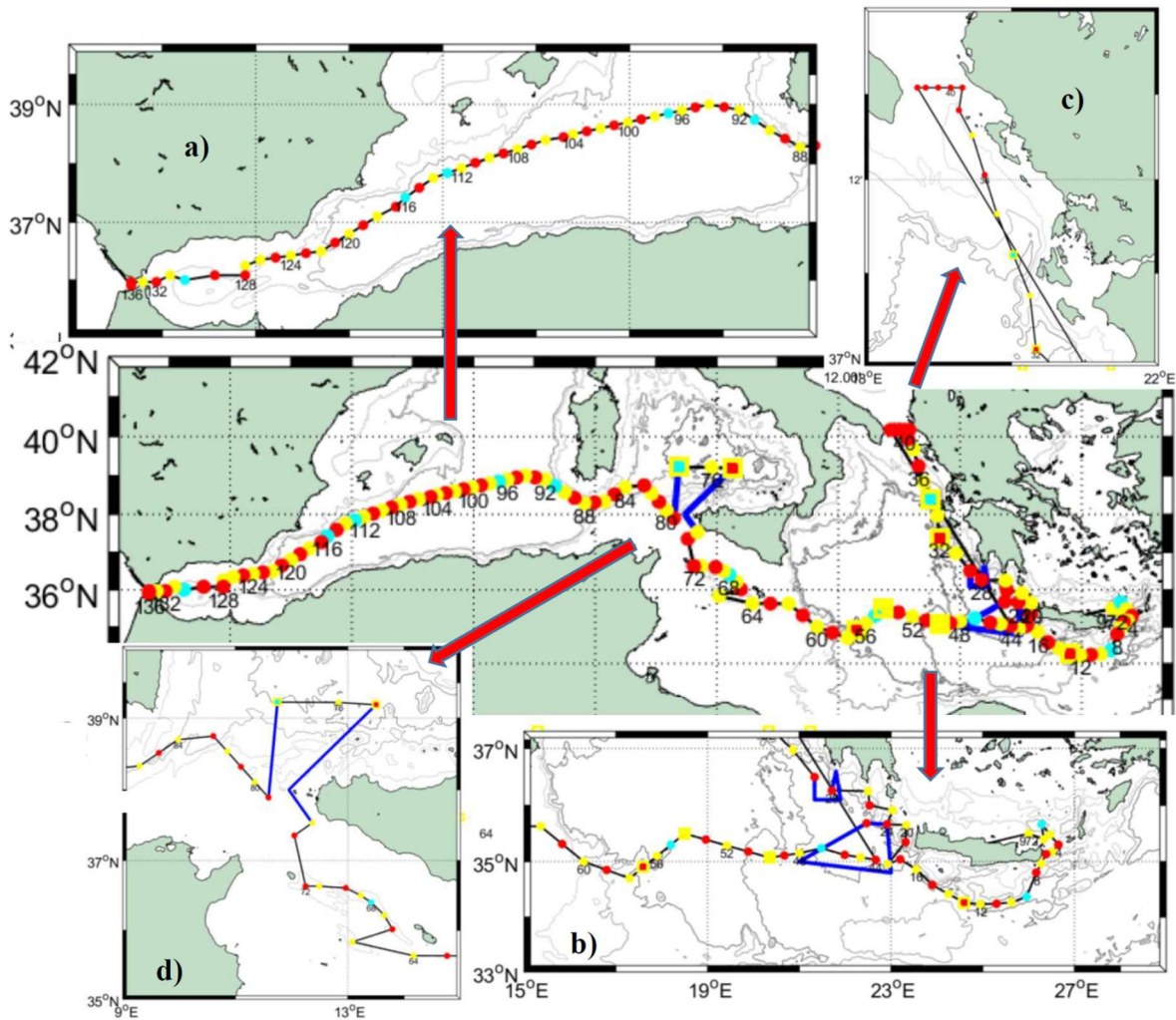
6 6. What are the baseline values of rarely measured Essential Ocean Variables (EOVs) such  
7 as dissolved organic carbon (DOC)?

8

## 9 **2. Data Provenance**

10 The survey was carried out on the German RV Maria S. MERIAN from 2<sup>nd</sup> of March to 3<sup>rd</sup> of  
11 April 2018. The cruise started on Iraklion, Greece and ended in Cadiz, Spain. The main focus  
12 of the cruise was on an east-west transect across the Western and Eastern Mediterranean Sea  
13 (figure 1) starting east of Crete and ending near the Strait of Gibraltar, which is a repeating  
14 hydrographic line in GO-SHIP (MED1). Difficulties with diplomatic authorizations for Marine  
15 Scientific Research (MSR) in the disputed EEZ between Greek and Turkey made it impossible  
16 for us to carry out measurements in this area, so that no data were obtained east of Kasos Strait.

17



1  
 2 Figure 1: Station Map. Yellow dots: CTD without any chemical sampling, red dots: CTD with  
 3 chemical sampling, cyan dots: CTD with chemical and additional sampling of isotopes, yellow  
 4 squares: deployment of drifter and floats, blue lines: fine resolved uCTD and ADCP tracks.  
 5 Black lines: Track with uCTD casts between CTD stations. a) Detail of the central map:  
 6 Western Mediterranean Sea. b) Detail of the central map: Eastern Mediterranean Sea. c) Detail  
 7 of the central map: Otranto Strait and northern Ionian Sea. d) Detail of the central map:  
 8 Tyrrhenian Sea and Strait of Sicily.

9  
 10 During the thirty-three days of the cruise we carried out measurements of hydrographic and  
 11 biogeochemical variables along-track with the classical approach i.e. CTD, IADCP, uCTD  
 12 instrumentation and bottle samples on highly resolved sections across the Mediterranean Sea.  
 13 The high resolution of CTD stations, enhanced for the physical parameters by additional uCTD  
 14 measurements, allowed us to resolve the eddy field on the sections, the analysis was also  
 15 supported and complemented by satellite data.



1 Most sections and CTD-positions follow previous sampling strategies (cruise M84 and other  
2 along the GO-SHIP line MED-01, i.e. Tanhua et al., 2013) to allow long-term trend analyses.  
3 Along the different sections, CTD stations including sampling of chemical parameters were  
4 conducted approximately every 30 nm, CTD without sampling about every 15-20 nm and with  
5 even smaller spacing in the Straits. In addition, underway CTD measurements and ADCP  
6 measurements were performed between CTD stations.

7 The water sampling program included measurements of all level 1 variables as defined by GO-  
8 SHIP (i.e. oxygen, macronutrients, transient tracers and the carbonate system, [http://www.go-  
9 ship.org/DatReq.html](http://www.go-ship.org/DatReq.html)) and measurements of the biogeochemical EOVs  $^{13}\text{C}$ , nitrous oxide  
10 ( $\text{N}_2\text{O}$ ) and dissolved organic carbon (DOC). These data were used to quantify trends and  
11 variability of ventilation and biogeochemical cycles, in particular uptake of anthropogenic  
12 carbon.

13 Sections were additionally conducted through the important passages: The Strait of Otranto,  
14 Kasos Strait, Antikythera Strait, Strait of Sicily and Strait of Gibraltar, in order to characterize  
15 the incoming and outgoing flows. CTD stations in the Eastern Ionian Sea were carried out to  
16 quantify the flow of the Levantine Surface Water (LSW) into the Adriatic Sea and to track the  
17 outflow of the Adriatic Deep Water (AdDW) into the Ionian Sea.

18

### 19 **3. Methods**

#### 20 **3.1 CTD/rosette**

21 Altogether 136 CTD cast were performed from which 18 catalogued as isotopic (a full suite of  
22 observations in Table 1a and b), 65 as chemical (i.e. GO-SHIP level 1 variables), and 59 as  
23 physical (i.e. only sampling for salinity). Due to the water amount needed, 2 casts were  
24 performed on most of the isotopic stations, the first cast was a full profile and the second a  
25 shallow one. During the physical stations water samples at 3 levels were taken for salinity  
26 analysis. The samples were then analyzed on board using a Guildline Autosal Salinometer. A  
27 total of 162 samples in 59 stations were taken during the cruise with an offset with respect to  
28 standard water varying from 0.0002 to 0.0030 depending on the laboratory temperature. The  
29 samples were taken at depth with a constant salinity gradient to ensure that no natural changes  
30 in salinity affect the comparison between sample and sensor.

31 The primary CTD system (specifications see table 2) initially used on board was a Seabird  
32 SBE9plus + CTD s/n 0285 from the University of Hamburg connected to a SBE11 deck unit,

1 configured with a 24- position SBE-32 pylon (from GEOMAR) with 10-liter Niskin bottles.  
 2 Position of bottles #23 and #24 was occupied by the IADCP (specifications see table 3).  
 3 Initially, the CTD was set up with two sensors for temperature and conductivity, an oxygen  
 4 sensor, a fluorometer and an altimeter. To test the configuration and performance of the  
 5 instrument a station was carried out on the Cretan Sea at the start of the cruise. Unfortunately,  
 6 we had countless problems with instruments, sensors, cables and rosette during most of the  
 7 campaign which forced us to change them very often with others available on board resulting  
 8 in a continuous change of system configuration. Thus, all different configurations were  
 9 carefully considered when post-processing the CTD data.

10 Temperature, salinity and pressure data were post-processed by applying Seabird software and  
 11 MATLAB® routines. At this stage, spikes were removed, 1 dbar averages calculated. A first  
 12 attempt to assess the performance of the conductivity sensors installed on the CTD-Rosette was  
 13 done by comparing the salinity data with the bottle samples analyzed with the salinometer. The  
 14 different hardware setups and configurations are taken carefully into account during post-  
 15 processing. Overall accuracies are within the expected range of salinity (0.003).

16

17 Table 2: Used CTD instrument and sensors. Owner of instruments are either the University of  
 18 Hamburg, Germany (IfM-HH), the National Institute of Oceanography and Geophysics (OGS),  
 19 Italy or the property of the vessel MERIAN (MSM).

<i>Instrument/Sensor</i>	<i>Serial Number (owner)</i>	<i>Calibration Date</i>
SBE 911plus / 917plus CTD	285 (IfM-HH)	03-Dec-14
	806 (MSM)	27-Jan-16
	807 (MSM)	08-Sep-15
Temperature 1: SBE-3-02/F	1717 (OGS)	22-Nov-17
	5716 (MSM)	15-Jul-17
Conductivity 1: SBE-4-02/2	3442 (OGS)	22-Nov-17
	4152 (MSM)	14-Jul-17
Temperature 2: SBE-3-02/F	1294 (IfM-HH)	11-Apr-17
	5719 (MSM)	15-Jul-17
Conductivity 2: SBE-4-02/2	1106 (IfM-HH)	12-Apr-17
	4156 (MSM)	14-Jul-17
Oxygen 1 SBE 43	3392 (OGS)	19-Dec-17
	2417 (MSM)	16-Aug-17
	0951 (MSM)	01-Dec-17
Oxygen 2 SBE 43	1761 (IfM-HH)	11-Apr-17
	2418 (MSM)	15-Aug-17
	0881 (MSM)	23-Dec-17

Fluorometer WETLAB	1755 (MSM)	18-Apr-17
	1754 (MSM)	21-Dec-17
SeaPoint (used on 1 station)	SCF2874	unknown
SPAR		10-Mar-16
PAR Chelsea		17-Oct-16

1  
2

### 3 **3.2 Underway-CTD**

4 Underway CTD measurements (uCTD, specifications see table 4) provide high-resolution  
5 profiles of temperature, conductivity and depth, which allow to characterize the upper ocean  
6 properties and to identify the position and characteristics of mesoscale structures. The  
7 advantage of this type of measurements is that it is not required to stop the vessel, but only to  
8 maintain lower velocities (about 3 kn) during the deployments to reach greater depths. These  
9 measurements were made with an Ocean Science uCTD system.

10 The first uCTD deployment was done on March 5<sup>th</sup>, between CTD 015 and 016 stations, and  
11 we continued with this type of sampling between each CTD station to increase the sampling  
12 resolution. Unfortunately, several deployments were cancelled due to severe weather conditions  
13 and no uCTD cast was performed when the depth was shallower than 500m. Altogether 176  
14 casts were taken with depths ranging from 557 to 864 m.

15 Two probes were used during the cruise with a no time limit mode configuration (apart from  
16 the first cast configured to stop recording after 600 seconds, reaching 616 m depth) in order to  
17 get longer records. The probe tail spools were attached to the winch through a rope loop that  
18 was made new every day in the morning. Despite the probes can record several casts, data were  
19 downloaded right after each cast using a SBE software in order to avoid losing the data in case  
20 the probe was lost, and to free the memory. The probes were exchanged when the battery was  
21 running low (around 3.8V). In three occasions, no data were recorded because the magnet was  
22 taken off twice before deployment.

23 For calibration purposes, some additional casts were done right after the CTD cast in order to  
24 compare the data sets. The probes were also sent down with the starboard CTD in station 130.

25 Data files were processed using a set of MATLAB® routines. After extracting the downcast  
26 data, a first correction was done for removing inaccuracies in the descend rate based on the  
27 work of Ullmann and Hebert (2013). Additionally, the data were aligned to the comparable  
28 CTD data sets.

29

1 Table 3: Used uCTD sensors.

<i>Probe 1</i>	<i>Device Type</i>	<i>Serial Number (owner)</i>
0289	90745 uCTD /SBE49 FastCat CTD	702-0289 (IfM-HH)
0183	90745 uCTD /SBE 49 FastCat CTD	702-0183 (IfM-HH)

2

3 **3.3 IADCP Measurements**

4 Ocean currents were studied by means of vertical profiles made with a IADCP-2 system  
 5 (Workhorse RD Instruments type, table 3) which included two ADCPs operating at a frequency  
 6 of 300 kHz, one looking upward and the other one looking downward. The system was placed  
 7 in the rosette occupying the position of Niskin bottles 23 and 24. During the cruise, the IADCP  
 8 batteries were changed twice: the first time on March 17<sup>th</sup> in Station 58 and the second time on  
 9 March 27<sup>th</sup> in Station 105. Except for three stations (station 73, 74, 80) with water depths less  
 10 than 500 m, IADCP measurements were done at all CTD. For these stations, the currents were  
 11 observed by the ship mounted ADCP. At isotope stations, IADCP profiles were only recorded  
 12 from the deep cast. The gained data were processed with LDEO MATLAB® IADCP-  
 13 processing system Version 10.15 (Turnherr, 2014). This software uses the raw IADCP data,  
 14 processed CTD data and navigational data from the CTD. The resulting data are the u- and v-  
 15 velocities at the depth. The bin size was set to 8m.

16

17 Table 4: Used IADCP.

Device Type	Serial Number (owner)
WHM300	Master s/n #22762 (IfM-HH)
WHM300	Slave s/n #22763 (IfM-HH)

18

19 **Shipborne ADCP**

20 During the whole campaign, underway current measurements were taken with two vessel-  
 21 mounted VM-ADCPs Ocean Surveyor (ADCP) manufactured by RDI. The first, with work  
 22 frequency of 75 kHz, covered approximately the top 500-700m of the water column. The  
 23 number of bins was set to 100 with bin size of 8 m. The second, with work frequency of 38  
 24 kHz, has a depth range of about 1600 m, set with the same bin number as the previous one and  
 25 bin size of 16 m. Both instruments run in narrowband mode and were controlled by computers  
 26 using the conventional RDI VMDAS software under a MS Windows system with a pinging set  
 27 to fast as possible. No interferences with other used acoustical instruments were observed. The

1 ADCP data was afterwards post-processed with the CODAS3 Software System  
2 ([https://currents.soest.hawaii.edu/docs/adcp\\_doc/](https://currents.soest.hawaii.edu/docs/adcp_doc/)), which allows extracting data, assigning  
3 coordinates, editing and correcting velocity data. Moreover, the data were corrected for errors  
4 in the value of sound velocity in water, and misalignment of the instrument with respect to the  
5 axis of the ship (about -2.8 degrees for 75 kHz ADCP and about -0.15 degrees for 38 kHz  
6 ADCP).

7

### 8 **3.5 Underway CO<sub>2</sub> and O<sub>2</sub> Measurements**

9 Underway (UW) measurements of partial pressure of CO<sub>2</sub> (pCO<sub>2</sub>), and dissolved oxygen partial  
10 pressure (pO<sub>2</sub>, the corresponding data set in Table 1b only contains pCO<sub>2</sub>) in seawater were  
11 carried out by means of a Contros HydroC pCO<sub>2</sub> analyzer for pCO<sub>2</sub> and an Aanderaa optode  
12 for oxygen.

13 The instruments were placed in a cooling box in the hangar. Seawater was drawn from the  
14 ship's centrifugal pump for clean seawater that was continuously flowing through the cooling  
15 box with the inlet close to the instruments. Water was pumped through a SeaBird 5 salinity and  
16 temperature sensor and on to the HydroC instrument (Gerke et al., 2020).

17 The system operated reliably throughout the cruise, except when data acquisition was  
18 interrupted for the pCO<sub>2</sub> instrument for 2 days directly after the ship's centrifugal pump was  
19 switched off. This led to a gap 5-days period without data between March 5<sup>th</sup> and 10<sup>th</sup>. During  
20 the cruise, 13 samples were taken from the cooling box for discrete measurements of pH and  
21 total alkalinity. The UW measurements started on March 2<sup>nd</sup> at 20:20 and stopped on April 1<sup>st</sup>,  
22 2018, at 14:00 (UTC).

23 The underway oxygen measurements were calibrated by comparing to the Winkler  
24 measurements taken for surface samples at the chemical CTD stations.

25

1 **3.6 Dissolved Oxygen**

2 Dissolved oxygen in seawater was not only measured with the CTD, but samples were also  
3 taken at every station and depth along the cruise and reported in  $\mu\text{mol/kg}$ . GO-SHIP guidelines  
4 recommend Winkler measurements on all samples, in addition to sensor measurements on the  
5 CTD-package, and we largely followed those recommendations. Unfortunately, we had to  
6 mark large numbers of oxygen values determined with the CTD as questionable due to the  
7 several technical problems with the CTDs and sensors. Usually, samples were taken at standard  
8 depths but specially at the surface and at the bottom the depths were varied according to the  
9 requirements of the other biogeochemical parameters. Oxygen was measured following the  
10 automatic Winkler potentiometric method modified after Langdon (2010). Titrations were done  
11 within the sampling calibrated flasks using an Automatic Titrator Mettler Toledo T50 with a  
12 platinum combined electrode.

13 Reagents blank and Thiosulphate standardization were done daily by means of Potassium Iodate  
14 Standard 1.667 millimolar by OSIL, UK. About 1400 samples were analyzed on board. The  
15 precision of dissolved oxygen measurements was determined on five replicates, at the  
16 beginning and at the end of the cruise (table 5).

17 In addition, during the cruise 46 duplicates were analyzed. The results are given in table 6.  
18

19

20 Table 5: Precision of dissolved oxygen. (STD = standard deviation, CV = Coefficient of  
21 Variation)

Parameter	<i>Beginning of the cruise</i>			<i>End of the cruise</i>		
	Mean $\mu\text{M}$	STD $\mu\text{M}$	CV%	Mean $\mu\text{M}$	STD $\mu\text{M}$	CV%
DISSOLVED OXYGEN	196.07	0.13	0.07	198.84	0.14	0.07

22

23

1 Table 6: Results of duplicates. <sup>(1)</sup>AD=|duplicate #1 – duplicate #2|; <sup>(2)</sup>RPD%=Absolute  
 2 Difference \*100/mean (dupl. #1, #2).

Parameter	Range μM	mean Absolute Difference <sup>(1)</sup> μM	mean Relative Percentage Difference <sup>(2)</sup>
DISSOLVED OXYGEN	179-240	0.18	0.09

3  
4

5 **3.7 Nutrients (nitrite, nitrate, phosphate, and silicate), Total Dissolved Nitrogen**  
 6 **(TDN) and Total Dissolved Phosphorus (TDP).**

7  
8

8 ***Nutrients***

9 Analyses were performed at 40 °C on a four-channel, Quattro SEAL Analytical Continuous  
 10 Flow Analyzer s/n 8014549; [https://www.seal-analytical.com/Products/SegmentedFlow](https://www.seal-analytical.com/Products/SegmentedFlowAnalyzers/QuAAtro39AutoAnalyzer/tabid/814/language/en-US/Default.aspx)  
 11 [Analyzers/QuAAtro39AutoAnalyzer/tabid/814/language/en-US/Default.aspx](https://www.seal-analytical.com/Products/SegmentedFlowAnalyzers/QuAAtro39AutoAnalyzer/tabid/814/language/en-US/Default.aspx), according to  
 12 Hansen and Koroleff (1999). Nitrite was determined through the formation of a reddish-purple  
 13 azo dye, and measured at 520 nm (SEAL Method No. Q-030-04 Rev. 2). Nitrate was reduced  
 14 to nitrite in a copperized cadmium reduction coil and then determined as described for nitrite  
 15 (SEAL Method No. Q-035-04 Rev. 4). The determination of phosphate was based on the  
 16 reduced blue phospho-molybdenum complex, and then measured at 880 nm (SEAL Method  
 17 No. Q-031-04 Rev. 1). Silicate was determined by means of acidic reduction of silicomolybdate  
 18 to molybdenum blue, then measured at 820 nm (SEAL Method No. Q-038-04 Rev. 0).

19 About 1400 nutrient samples were analyzed on board. The onboard precision of nutrient  
 20 measurements was determined on five replicates, at the beginning and at the end of the cruise.  
 21 The results are shown in table 7.

22 In addition, during the cruise 140 duplicates were analyzed. The results are shown in table 8.

23 An internal quality check was daily performed by means of analyses of QUASIMEME samples,  
 24 which provided results within the already certified ranges.

25  
26

1 Table 7: On board precision of nutrient measurements

Parameter	Beginning of the cruise			End of the cruise		
	Mean μM	STD μM	CV%	Mean μM	STD μM	CV%
NITRITE (1)	0.01	0.01	100	0.03	0.01	56.5
NITRITE + NITRATE	4.94	0.01	0.2	9.01	0.02	0.2
PHOSPHATE	0.18	0.01	5.5	0.41	0.01	3.1
SILICATE	8.34	0.03	0.3	9.55	0.04	0.5

2

3 Table 8: Analysis of duplicates. (1)AD=|duplicate #1 – duplicate #2|; (2) RPD%=Absolute  
4 Difference \*100/mean (dupl. #1, #2); (3) Nitrite statistics was given just for completeness,  
5 since the concentration levels recorded were too low, often below the detection limit.

Parameter	Range μM	mean Absolute Difference (1) μM	mean Relative Percentage Difference (2)
NITRITE (3)	0-0.19	0.01	48.77
NITRITE+NITRATE	0.33-9.86	0.02	0.42
PHOSPHATE	0-0.47	0.01	5.13
SILICATE	0.93-11.00	0.04	0.72

6  
7



1 **TDN and TDP**

2 About 550 samples for Total Dissolved Nitrogen and Total Dissolved Phosphorus (TDN and  
3 TDP) on land-based laboratory analyses were collected and frozen at -20°C after filtration on  
4 pre-combusted GF/F filter. The dissolved organic components, Dissolved Organic Nitrogen  
5 (DON) and Dissolved Organic Phosphorus (DOP) were subsequently calculated by subtracting  
6 their mineral constituents (NO<sub>3</sub>+NO<sub>2</sub>) and PO<sub>4</sub>, respectively.

7

8 **3.8 Discrete CO<sub>2</sub> System Measurements**

9 Discrete CO<sub>2</sub> variables were measured on board, being Dissolved Inorganic Carbon (DIC), pH,  
10 Total Alkalinity (TA) and carbonate ion (CO<sub>3</sub><sup>2-</sup>) at selected stations and depths (table 9). In  
11 addition, discrete samples for DIC, pH and TA were analyzed specifically from surface Niskin  
12 bottles to be compared with the continuous water supply feeding the pCO<sub>2</sub> system in determined  
13 stations. For further details, see Hainbucher et al. (2018).

14

15 Table 9: Total number of CO<sub>2</sub> system samples analyzed during the MSM72 cruise. Total  
16 number of fired bottles 1723.

	DIC	pH	TA	CO <sub>3</sub> <sup>2-</sup>	Surface
<b>Samples</b>	479	1160	949	391	22

17

18 **DIC**

19 Samples for DIC were collected following transient tracers and dissolved oxygen, in 500 ml  
20 borosilicate bottles following standard procedures. No poison was added. Samples were left at  
21 room temperature in the dark until analysis, maximum 48 hours after collection. DIC samples  
22 were analyzed with a MARIANDA VINDTA 3D system coupled with a UIC 5011 coulometer.  
23 This analysis overall consists of extracting seawater CO<sub>2</sub> from a known volume of sample by  
24 adding phosphoric acid, followed by coulometric detection (Johnson et al., 1993). No  
25 calibration unit was available for the system. A new coulometric cell was prepared for every  
26 batch of analysis and the accuracy of the DIC measurements was assessed by using Certified  
27 Reference Material (CRM #158 & #170 provided by Prof. Dickson, UCSD). The calibration  
28 factor obtained from the CRM was used for adjusting the final DIC of each sample measured  
29 in the corresponding batch of analysis. In addition, substandard seawater (stabilized seawater  
30 from the Cretan Sea 700m salinity minimum, stored in the dark in a 30 L container) was  
31 analysed at the beginning and end of the batch analysis as a secondary quality control. The

1 precision of the DIC measurements was checked by: 1) double analysis from the same sample  
2 and 2) replicate analysis from 4 to 5 samples collected from the same Niskin bottle. The  
3 precision is estimated to be  $1 \mu\text{mol kg}^{-1}$  and the accuracy  $2 \mu\text{mol kg}^{-1}$ .

## 4 5 **pH**

6 Seawater spectrophotometric pH was measured following Clayton and Byrne (1993) at almost  
7 all depths in the chemical and isotope stations during the MSM72 cruise (Table 1). This method  
8 consists on adding a volume of indicator solution to the seawater sample, so that measuring the  
9 absorbance of the sample at different wavelengths and obtaining the ratio between two of the  
10 wavelength's absorbance is proportional to the sample pH. The indicator was a 2 mM solution  
11 of unpurified *m*-cresol purple (Sigma Aldrich®) prepared in seawater and maintained at dark,  
12 with no air contact (Absorbance Ratio 1.30). Samples were taken following standard procedures  
13 immediately after DIC and directly into cylindrical 10 cm path length optical glass cells. The  
14 cells were thermostated at  $25 \pm 0.2^\circ\text{C}$  during one hour before analysis. Absorbance  
15 measurements were obtained in the thermostated chamber of a double beam UV 2600 Shimadzu  
16 spectrophotometer. The equipment was checked before the cruise for the absorbance and  
17 wavelength accuracy using holmium standards. pH values on the total scale were calculated  
18 and referred at  $25^\circ\text{C}$  by using the formula by Clayton and Byrne (1993). The injection of the  
19 indicator in the sample slightly changes the sample pH. Following standard operating  
20 procedures, double additions of the indicator were performed over a pH gradient in order to  
21 obtain the corresponding correction (Hainbucher et al., 2018). The pH accuracy was controlled  
22 measuring TRIS buffer solution samples (batch #72, provided by Prof. Dickson, UCSD). TRIS  
23 samples were stabilized at three different temperatures covering the pH range found during the  
24 MSM72 cruise. Differences between measured and theoretical TRIS pH varied between 0.009  
25 to 0.005. The pH precision was checked by replicate analysis from cells collected at the same  
26 Niskin from surface and deep waters. The precision is estimated to be 0.0004 pH units and the  
27 accuracy 0.005 pH units. During the cruise, some samples were also analyzed with purified *m*-  
28 cresol purple provided by Prof. Byrne (USC).

## 29 30 **TA**

31 TA was analyzed following a double end point potentiometric technique by Pérez and Fraga  
32 (1987) further improved by Pérez et al. (2000). This technique is faster than the whole curve  
33 titration, with comparable results (Mintrop et al., 2000). TA was measured at most stations and

1 depths (Table 1). Seawater samples for TA were collected after pH samples in 600 ml  
2 borosilicate bottles following standard procedures. Samples were left at room temperature in  
3 the dark until analysis, maximum 48 hours after collection. TA was measured by titration with  
4 0.1 N hydrochloric acid dispensed with an automatic potentiometric titrator, Titrand  
5 Metrohm®, provided with a combination glass electrode coupled with a temperature probe. The  
6 electrode was standardized using a 4.41 pH ftalate buffer made in CO<sub>2</sub> free seawater. The TA  
7 accuracy was assessed with CO<sub>2</sub> CRM (batch #170, provided by Prof. Dickson, UCSD) In  
8 addition to the CRM calibration, a drift control was conducted by analyzing substandard  
9 seawater (big volume of seawater stored in the dark, as for DIC) at the beginning and at the end  
10 of the analysis session. Each sample was measured twice and the mean value is reported, with  
11 the mean standard deviation of all duplicate differences being 0.6 μmol kg<sup>-1</sup>. In addition, typical  
12 reproducibility analysis were performed from samples collected from the same niskin bottle at  
13 different stations along the cruise. The TA precision is estimated to be 1 μmol kg<sup>-1</sup> and the  
14 accuracy 2 μmol kg<sup>-1</sup>.

### 15 **CO<sub>3</sub><sup>2-</sup>**

16 The CO<sub>3</sub><sup>2-</sup> ion concentration was determined spectrophotometrically following Byrne and Yao  
17 (2008) incorporating the recent improvements by Patsavas et al. (2015), at selected stations and  
18 depths (Table 1) Samples for CO<sub>3</sub><sup>2-</sup> were collected after TA following the same procedure as  
19 for pH but within cylindrical optical quartz 10 cm path length cuvettes. The cells were stabilized  
20 at 25°C for one hour before the analysis, maximum 24 hours after collection. A solution of  
21 0.022 M of Pb (ClO<sub>4</sub>)<sub>2</sub> was added to the seawater sample and the PbCO<sub>3</sub> complex formed  
22 afterwards was detected spectrophotometrically in the UV spectra. Absorbance measurements  
23 were obtained in the thermostated chamber of a double beam UV 2600 Shimadzu  
24 spectrophotometer. The equipment was checked before the cruise for the absorbance and  
25 wavelength accuracy width using holmium standards. The CO<sub>3</sub><sup>2-</sup> in μmol kg<sup>-1</sup> is the  
26 concentration of ion carbonate at 25°C calculated using the formula by Patsavas et al.  
27 (2015). The CO<sub>3</sub><sup>2-</sup> precision was checked by replicate analysis from cells collected at the same  
28 niskin from surface and deep waters. It is estimated to be 1 μmol kg<sup>-1</sup>.

29

### 30 **3.9 Measurements of CFC-12 and SF<sub>6</sub>**

31 During the cruise, one gas chromatograph purge-and-trap (GC/PT) system was used for the  
32 measurements of the transient tracers CFC-12 and SF<sub>6</sub>. The system is modified versions of the  
33 set-up normally used for the analysis of CFCs (Bullister and Weiss, 1988). All samples were

1 collected in 250 mL ground glass syringes, of which an aliquot about 200 mL was injected to  
2 the purge-and-trap system, normally within 5 hours from sampling.

3 The traps consisted of 100 cm 1/16" tubing packed with 70cm Heysep D kept at temperatures  
4 between -70 and -75°C during trapping. The traps were desorbed by heating to 120°C and  
5 passed onto the pre-column. The pre-column consisted of 20 cm Porasil C followed by 20 cm  
6 Molsieve 5A in a 1/8" stainless steel column. The main column was a 1/8" packed column  
7 consisting of 180 cm Carbograph 1AC (60-80 mesh) and a 50 cm Molsieve 5A post-column.  
8 Both columns were kept isothermal at 60°C. Detection was performed on an Electron Capture  
9 Detector (ECD).

10 Standardization was performed by injecting small volumes of gaseous standard containing  
11 CFC-12 and SF<sub>6</sub>. This working standard was prepared by the company Dueste-Steiniger (DS1.).  
12 The CFC-12 and SF<sub>6</sub> concentrations in the working-standard has been calibrated vs. a reference  
13 standard obtained from R.F Weiss group at SIO, and the CFC-12 data are reported on the SIO98  
14 scale. Calibration curves were measured roughly once a week in order to characterize the non-  
15 linearity of the system, depending on workload and system performance. Point calibrations  
16 were always performed between stations to determine the short-term drift in the detector.  
17 Replicate measurements were taken except for near coastal stations due to high workload. To  
18 assess the reproducibility of the set-up, 50 replicates samples were run, and resulted in a  
19 reproducibility of 1.0 % or 0.01 pmol kg<sup>-1</sup> for CFC-12 and 2.3% or 0.03 fmol kg<sup>-1</sup> for SF<sub>6</sub>. In  
20 total, we successfully measured 1084 samples on 68 stations for transient tracers. The results  
21 are discussed in Li and Tanhua (2020).

22 In addition to the on-board analysis, on three stations (#52, #84, and #106) 1500 ml glass  
23 ampoules were flame sealed for later analysis in the lab in Kiel for the detection of novel  
24 halogenated tracers such as HFC134a and HCFC22 (Li and Tanhua, 2019).

25

### 26 **3.10 Dissolved Organic Carbon (DOC)**

27 Seawater samples for DOC were collected from the CTD-Rosette into 250 ml Polycarbonate  
28 Nalgene bottles. Samples were filtered through a 0.2 µm Nylon filter under high-purity air  
29 pressure. Filtered samples were collected in 60 ml Nalgene bottles, acidified and stored at 4°C  
30 and in the dark.

31 DOC measurements were carried out with a Shimadzu Total Organic Carbon analyzer (TOC-  
32 Vcsn), by high temperature catalytic oxidation. Samples were acidified with HCl 2N and

1 sparged for 3 minutes with CO<sub>2</sub>-free pure air, in order to remove inorganic carbon. From 3 to 5  
2 replicate injections were performed until the analytical precision was lower than 1% ( $\pm 1\mu\text{M}$ ).  
3 A five-point calibration curve was done by injecting standard solutions of potassium hydrogen  
4 phthalate in the expected concentration range of the samples. At the beginning and end of each  
5 analytical day the system blank was measured using low carbon water (LCW) and the reliability  
6 of measurements was controlled by comparison of data with a DOC reference (CRM) seawater  
7 sample kindly provided by Prof. D.A. Hansell of the University of Miami  
8 (<http://yyy.rsmas.miami.edu/groups/biogeochem/CRM.html>).

9 In total 650 samples were collected in 38 stations. Samples were collected at the following  
10 depths: 10, 25, 50, 75, 100, 150, 200, 300, 400, 500, 750, 1000 and every 250 m until the  
11 bottom.

12

### 13 **3.11 Chromophoric dissolved organic matter (CDOM)**

14 Chromophoric dissolved organic matter (CDOM) is the fraction of DOM that absorbs light at  
15 visible and ultraviolet (UV) wavelengths. It plays a key role in the marine ecosystem by  
16 regulating light penetration into the water column (Nelson and Siegel, 2013) and preventing  
17 cellular DNA damage (Herndl et al., 1993; Häder and Sinha, 2005). A fraction of CDOM re-  
18 emit part of the absorbed light and is called fluorescent DOM (FDOM). The study of the  
19 absorption properties of CDOM, together with the analysis of the excitation-emission matrixes  
20 (EEMs) through the parallel factorial analysis (PARAFAC) can give qualitative information on  
21 the different groups of chromophores (protein-like, humic-like and PAH-like) present in the  
22 DOM pool, their changes due to photodegradation and/or microbial transformation, the main  
23 sources of CDOM and an indirect estimation of its molecular weight and aromaticity degree  
24 (Stedmon and Nelson, 2015, Retelletti et al., 2015, Gonelli et al., 2016, Margolin et al., 2018).  
25 The CDOM data collected during the MSM72 cruise will represent an unique opportunity to:  
26 (i) Compare CDOM optical properties in the different water masses of the Mediterranean Sea  
27 with those collected in the GEOTRACES cruise (Spring-summer 2013) and to relate them to  
28 the different trophic conditions of the basin; (ii) Study the relationship between DOC and  
29 CDOM in the surface, intermediate and deep waters.

30

### 1 **3.12 Sampling for Measurements of Stable Carbon Isotopes on Dissolved** 2 **Inorganic Carbon (DIC)**

3 Samples for the determination of stable carbon isotopes ( $\delta^{13}\text{C}$ ) of Dissolved Inorganic Carbon  
4 (DIC) were taken on 11 stations (the “isotope stations”, normally performed as a double cast)  
5 in the various basins along the cruise-track. In total 214 samples were taken in 100 ml dark  
6 glass bottles immediately poisoned with 100  $\mu\text{L}$  saturated mercury chloride. The samples were  
7 measured off-line during fall of 2018 at the Centre for Isotope Research (CIO), Energy and  
8 Sustainability Research Institute Groningen (ESRIG), University of Groningen.

### 9 10 **3.13 $\text{NO}_3^-$ isotopes ( $\delta^{15}\text{N}$ & $\delta^{18}\text{O}$ )**

11 Samples for nitrogen (N) and oxygen (O) isotopes in nitrate ( $\text{NO}_3^-$ ) and nitrate+nitrite ( $\text{NO}_3^-$   
12  $+\text{NO}_2^-$ ) analysis were collected at 44 stations evenly distributed along the transect. In total, 790  
13 samples have been collected. High-resolution  $\text{NO}_3^-$   $\delta^{15}\text{N}$  and  $\delta^{18}\text{O}$  measurements represent a  
14 powerful tool to unravel the sources and sinks of reactive (i.e., fixed) N at the scale of the  
15 Mediterranean Sea. Complemented with coral-bound  $\delta^{15}\text{N}$  records covering the last centuries,  
16 these measurements may also shed light on the contribution of industrially fixed N to the  
17 reactive N budget, by revealing the large-scale systematics required to interpret the records back  
18 in time.

19 Unfiltered samples for N and O isotopic composition of  $\text{NO}_3^-$  were collected in 60 mL plastic  
20 bottles and stored frozen ( $-20^\circ\text{C}$ ) until analysis.  $\text{NO}_3^-+\text{NO}_2^-$   $\delta^{15}\text{N}$  and  $\delta^{18}\text{O}$  will be measured  
21 (2019-2020) at the Max Planck Institute using the denitrifier method (Sigman et al., 2001;  
22 Casciotti et al., 2002). Briefly, 3-20 nmol of  $\text{NO}_3^-+\text{NO}_2^-$  is quantitatively converted to  $\text{N}_2\text{O}$  gas  
23 by denitrifying bacteria (*Pseudomonas aureofaciens*) that lack an active  $\text{N}_2\text{O}$  reductase. The  
24  $\text{N}_2\text{O}$  is then analyzed by gas chromatography-isotope ratio mass spectrometer (GC-IRMS;  
25 MAT253, Thermo) with on-line cryo-trapping (Weigand et al., 2016). Measurements are  
26 referenced to air  $\text{N}_2$  for  $\delta^{15}\text{N}$  and VSMOW for  $\delta^{18}\text{O}$  using the nitrate reference materials IAEA-  
27  $\text{NO}_3$  and USGS-34. For  $\text{NO}_3^-$   $\delta^{15}\text{N}$  and  $\delta^{18}\text{O}$  analysis,  $\text{NO}_2^-$  is removed with the sulfamic acid  
28 method prior to the isotopic analysis (Granger and Sigman, 2009). The reproducibility is  
29 generally better than 0.1‰ for  $\delta^{15}\text{N}$  and  $\delta^{18}\text{O}$ , respectively.

### 30 31 **3.14 LISST – DEEP**

32 The LISST-Deep instrument obtains in-situ measurements of particle size distribution, optical  
33 transmission, and the optical volume scattering function (VSF) at depths down to 3,000 meters.

1 It is manufactured by Sequoia Inc., and owned by the Hellenic Centre for Marine Research  
2 (HCMR) – Greece.

3 Using a red 670nm diode laser and a custom silicon detector, small-angle scattering from  
4 suspended particles is sensed at 32 specific log-spaced angle ranges. This primary measurement  
5 is post-processed to obtain sediment size distribution, volume concentration, optical  
6 transmission, and volume scattering function. The LISST-Deep s/n 4004 is categorized as a  
7 type B instrument, which means that the range of particles it measures ranges from 1.25  $\mu\text{m}$  to  
8 250  $\mu\text{m}$ . The LISST-Deep must be powered externally at all times. This is typically achieved  
9 by connecting it to a rosette, getting power from the main CTD unit.

10 Parameters measured during the cruise were:

- 11 • Particle size distribution from 1.25-250 $\mu\text{m}$  or 2.5-500 $\mu\text{m}$
- 12 • Depth (3000 m max depth @ 0.8 m resolution)
- 13 • Optical transmission @ 0.1 % resolution
- 14 • Beam attenuation Coefficient @ 0.1  $\text{m}^{-1}$  resolution
- 15 • Volume concentration @ 0.1  $\mu\text{l/l}$  resolution
- 16 • Volume scattering function (VSF)

17 The measurement of these parameters provided important information on the number, size and  
18 quality (phytoplankton, sediment, etc.) of the suspended matter in the water column. Further  
19 information for the determination of water masses was provided by the estimation of the  
20 intrinsic optical properties. Finally, for the first  $\sim 100\text{m}$  we estimated the color of the sea and  
21 compared this estimation with satellite images, providing valuable information for the  
22 calibration of satellite algorithms.

23 For the cruise MSM72 the sampling of these optical estimates is in itself an important  
24 achievement because, for the first time LISST – DEEP was used to record data in a transect  
25 over the full length of the Mediterranean Sea. Furthermore, the estimation of these parameters  
26 combined with POC - PON estimation, and other physical and chemical parameters, improve  
27 the study of the dynamics of the Mediterranean Sea.

28 In general, the use of LISST – DEEP during the cruise follows the standard methods, which are  
29 provided by Sequoia Inc., but with one important difference. For the estimation of the above  
30 parameters the use of a background file is required for normalization purposes. This file is  
31 normally produced in laboratory conditions with MilliQ 2 filtered water. However, experience

1 until now has proved that especially in the eastern Mediterranean Sea (which is characterized  
2 as ultra-oligotrophic) the use of this background file leads us to an overestimation of the  
3 parameters and especially of the beam attenuation coefficient. Therefore, during this cruise we  
4 used a sampled in situ background file chosen as the minimum of the sum of the digital counts  
5 in the 32 rings and where the LaserPower to LaserReference (Lp/Lr) ratio is maximum.

6 The main problem, which we faced, was the frequent change of the CTD main unit and the  
7 different cables that we had to use for the instrument connection to the CTD. Fortunately, with  
8 the most valuable help of the cruise technician we managed to deploy the LISST – DEEP as  
9 much as possible. Additionally, the maximum depth limitation of the instrument (3000m)  
10 enforced us to remove it in deep casts achieving a total of 54 stations.

11

## 12 **4. Discussion and Conclusion**

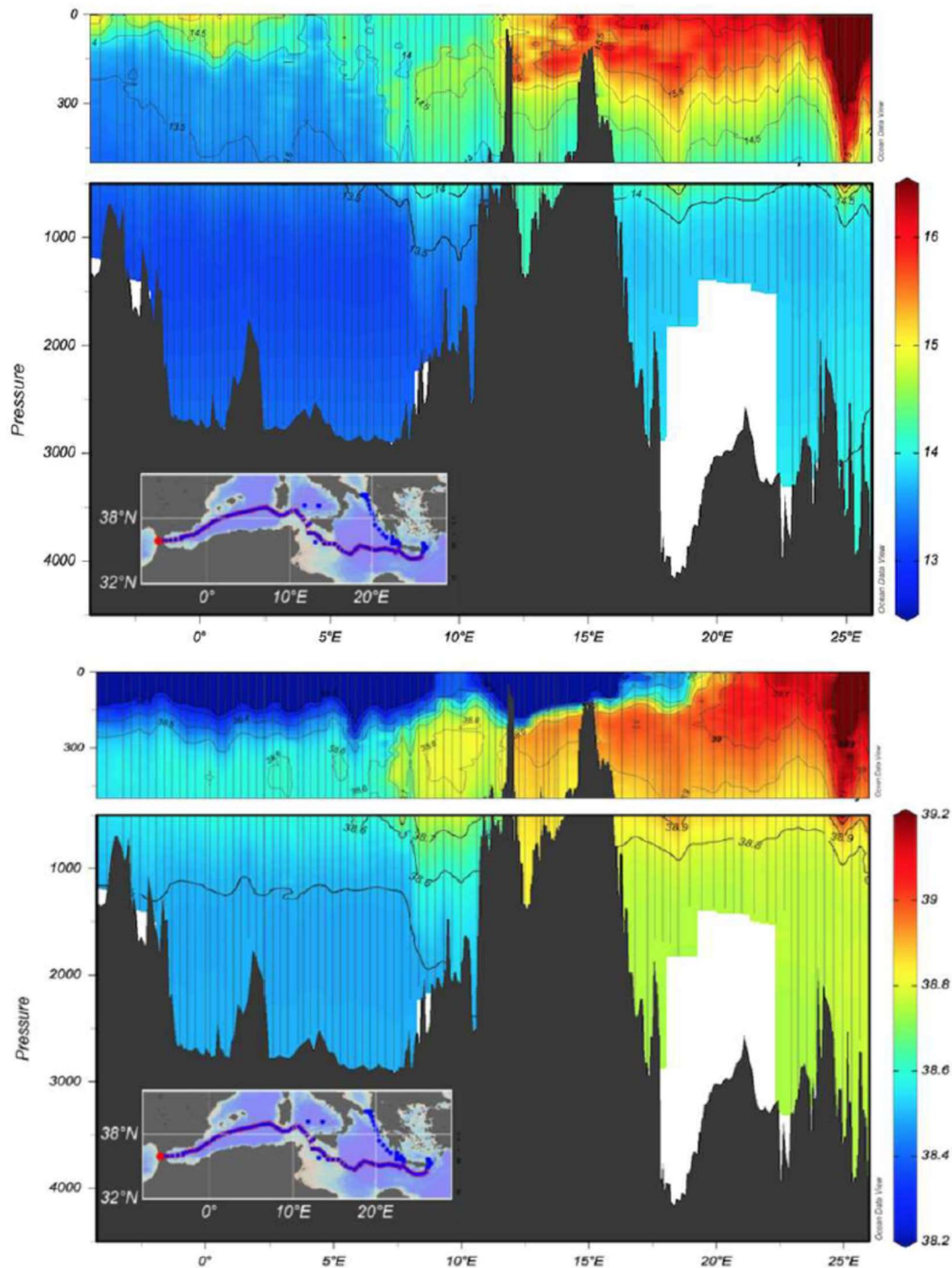
13 Discussion and conclusion will focus in this publication on the quality of the data of MSM72  
14 cruise. We will concentrate here on the basic physical and biogeochemical parameters, as  
15 selected examples, to show the relevance of the sampled data and so as to be able to answer the  
16 questions on the scale and variability of the circulation and biogeochemical cycle in the  
17 Mediterranean Sea (see Introduction).

18

### 19 **4.1 Physical parameters**

20 The west east section (figure 2) is a typical example for the distribution of temperature and  
21 salinity in the Mediterranean Sea showing the different heat and salt content between the  
22 western and eastern basin. A clear intrusion of the salty Levantine Intermediate Water (LIW)  
23 from east to west in the first 500m is depicted while the low salinity Atlantic Water (AW)  
24 protrudes eastwards creating a front at about 20-22°E.



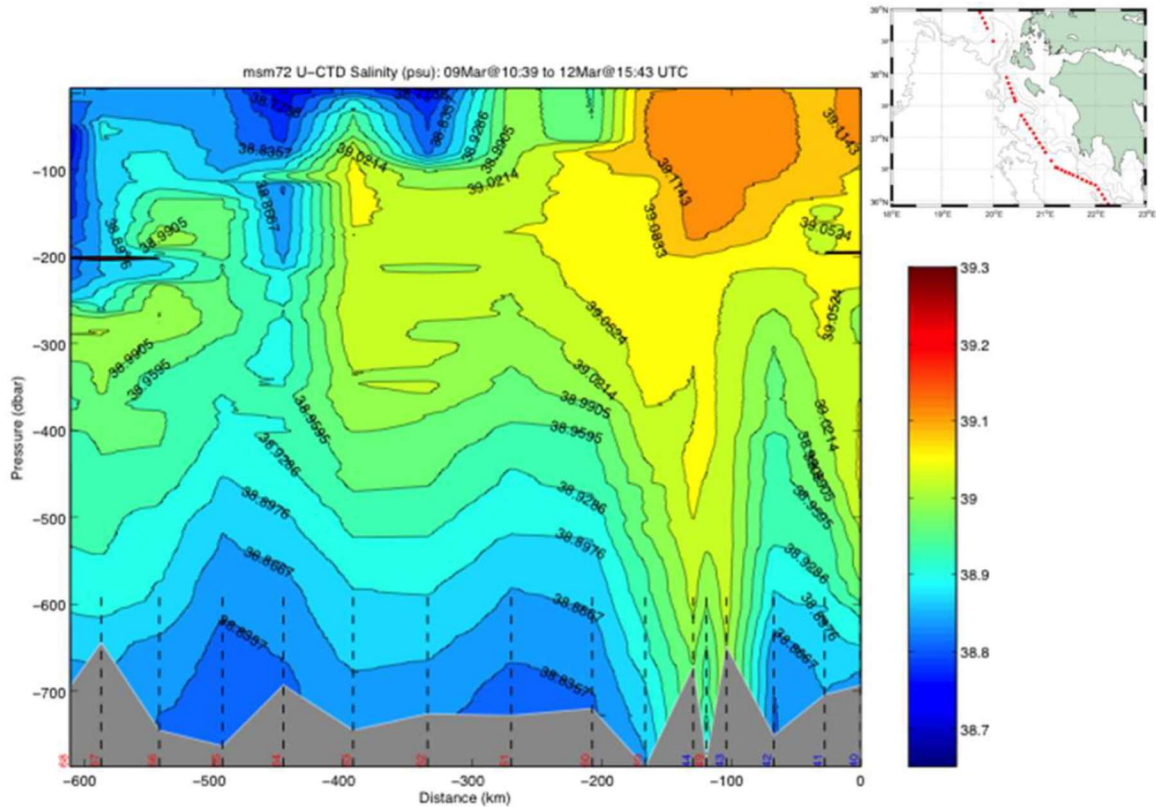


1  
2  
3  
4  
5

Figure 2: West-east temperature (top) and salinity (below) sections through the Mediterranean Sea.

6 The underway CTD data are a valuable addition to the classical CTD data. They enhance the  
7 resolution of data in the horizontal scale and give insight in eddy activity. Although the data do  
8 not reach to the bottom, the vertical resolution with about 1000 m is useful to characterize scales  
9 relevant for the LIW transport.

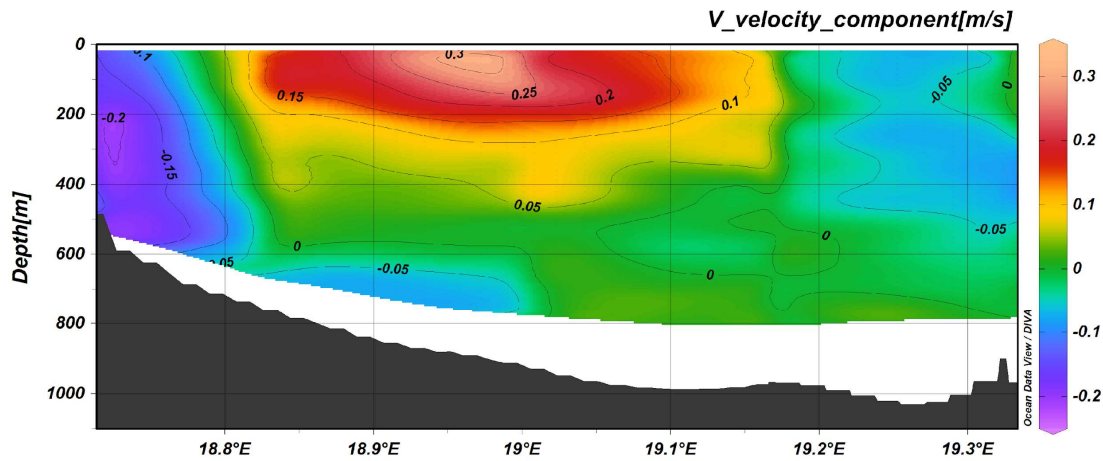
1 The uCTD stations along the easternmost part of the northward transit in the Ionian Sea are  
2 taken in average every 5 nm. Larger gaps in the line were essentially caused by the deployment  
3 of CTD stations. The uCTD salinity distribution of figure 3 shows that the Pelops gyre is well  
4 resolved.



5

6 Figure 3: uCTD salinity transect. Location is shown in the upper right panel.

7 Considering the route of the ship during the cruise, it was possible to identify different ADCP  
8 transects that correspond to areas with the most important water mass dynamics. In particular  
9 the most important sections were: gyre activity in the area west of Crete and south of  
10 Peloponnese, the west Cretan, Otranto (figure 4) and Sicily Straits, the east boundary of the  
11 Ionian Sea and the west-east Mediterranean transect. The north-south current component (figure  
12 4) in the Strait of Otranto clearly shows the outflow of the Adriatic Deep Water (AdDW) along  
13 the western part while in the upper and intermediate layer of the central part the inflow of the  
14 Levantine Intermediate Water (LIW) proceeds.



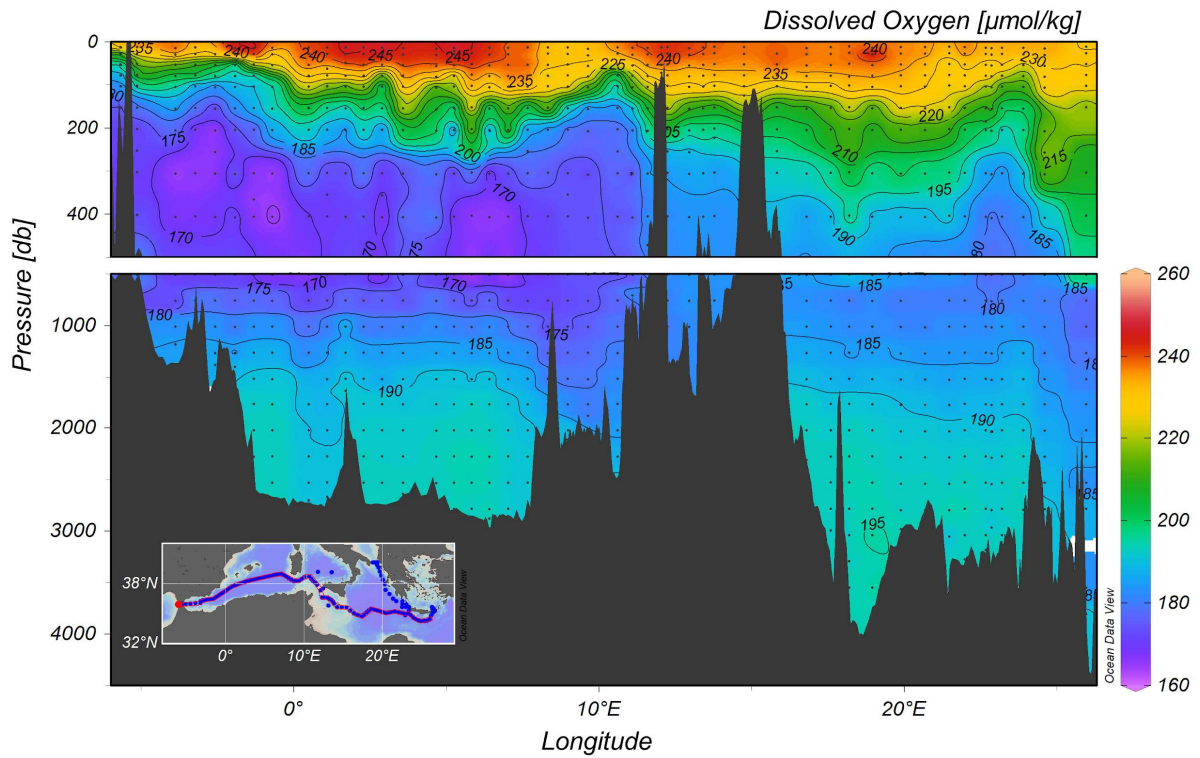
1  
2 Figure 4: Transect across the Strait of Otranto from ADCP 38, positive numbers correspond to  
3 northward currents.

4

5

## 6 **4.2 Biogeochemical parameters**

7 The vertical distribution of dissolved oxygen along a section from the Cretan Sea to Gibraltar,  
8 including part of the Cretan Passage and the southern Ionian is shown in figure 5. This section  
9 shows the Oxygen Minimum Layer ( $<180 \mu\text{moles/kg}$ ) which occupies the layer 500-1500m.  
10 Increased oxygen towards the bottom indicate the ventilation of deep water in the  
11 Mediterranean. The western part of the Ionian Sea appears to be better oxygenated than the  
12 eastern part due to the spreading of newly ventilated dense water from the Adriatic Sea via the  
13 Otranto Strait – a feature that is observed in the transient tracer section as well.

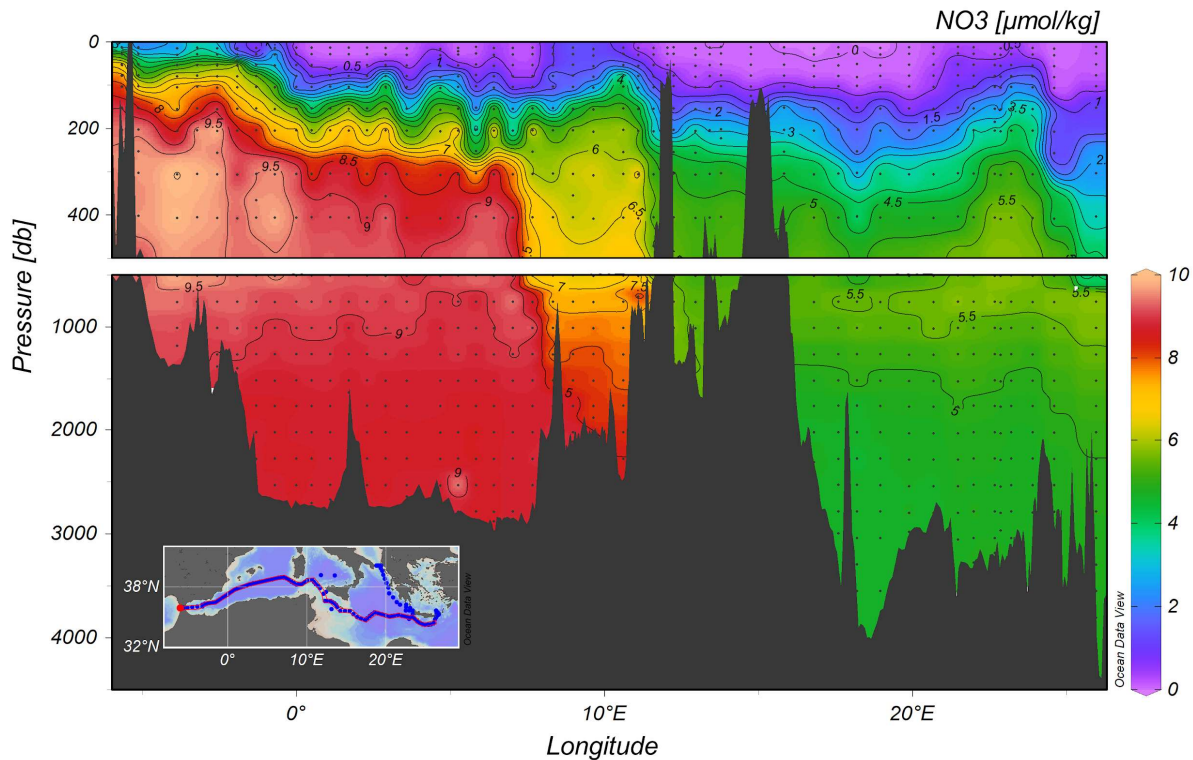


1

2 Figure 5: Distribution of dissolved oxygen along the trans-Mediterranean section.

3

4 Figure 6 illustrates the distribution of nitrate along the quasi-zonal section. Interesting features  
 5 include: the maximum nutrient layer in the range of depth of 500-1500 m which is co-located  
 6 to the minimum of transient tracers; the deepest layer shows an homogeneous distribution of  
 7 nutrients and the nutrient impoverished upper layer is, not yet completely depleted of nutrients,  
 8 likely do to subject to mesoscale dynamics (as, for example, south of Crete).



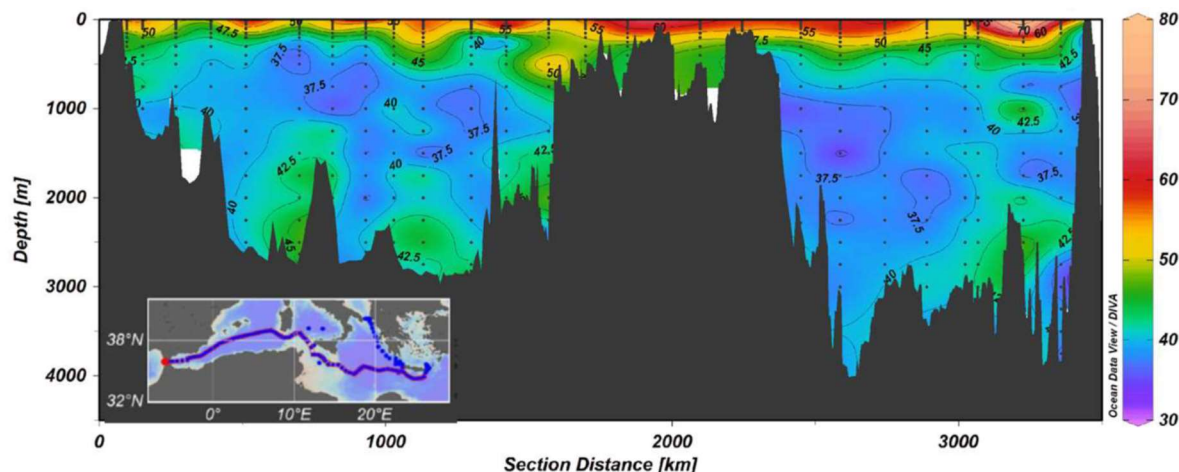
1

2 Figure 6: Distribution of nitrate along the trans-Mediterranean section.

3

4 The DOC data collected during the MSM72 cruise represents an unique opportunity to (i)  
 5 investigate the long-term variation in DOC distribution in intermediate and deep waters on a  
 6 basin scale; (ii) quantify the role of DOC in C export and sequestration in the Mediterranean  
 7 Sea; (iv) estimate DOC mineralization rates; (v) asses the functioning of microbial loop in the  
 8 different areas of the Mediterranean Sea.

9 DOC concentrations range between 34 and 80  $\mu\text{M}$  (figure 7). The highest values ( $> 50 \mu\text{M}$ )  
 10 were observed in the upper 200 m, with a marked increase moving eastward. The lowest  
 11 concentrations ( $< 40 \mu\text{M}$ ) are between 1000 and 2000 m, in the bottom waters a slight increase  
 12 in DOC can be observed. This feature, already reported for the Mediterranean Sea, can be  
 13 explained by the export of the DOC accumulated in the surface layer by deep water formation  
 14 (Santinelli, 2015 and references herein). The high stratification, occurring in the easternmost  
 15 stations, makes DOC accumulation there more visible. A different functioning of the microbial  
 16 loop has been reported for the western and eastern Mediterranean Sea and these data support  
 17 that DOC dynamics in the surface layer of the two sub-basins is different.



1

2 Figure 7: DOC vertical distribution along the trans-Mediterranean section

3

#### 4 **5. Data access**

5 Data are published at the information system PANGAEA and CCHDO;

6

#### 7 **6. Acknowledgements**

8 We thank Captain Björn Maaß, his officers and the crew of R/V MARIA S. MERIAN for the  
9 support of our scientific program, for their unending competent and friendly help.

10 The financial support for the cruise was provided by the project of the “Deutsche  
11 Forschungsgemeinschaft” U4600DFG040204. We gratefully acknowledge their support.

12 The CO<sub>2</sub> team was funded by an internal IEO grant MEDSHIP18, A.E.R. Hassoun was funded  
13 by a POGO grant. The OGS team was funded by an internal grant.

14

#### 15 **7. References**

16 Bullister, J. L., and Weiss, R. F.: Determination of CCl<sub>3</sub>F and CCl<sub>2</sub>F<sub>2</sub> in seawater and air,  
17 Deep-Sea Res., 35, 839-853. 1988.

18 Byrne, R. H., and Yao, W.: Procedures for measurement of carbonate ion concentrations in  
19 seawater by direct espectral photometric observations of Pb (II) complexation. Mar. Chem., 112  
20 (1–2), 128–135, 2008.

21 Carlson, C.A. and Hansell, D.A.: Biogeochemistry of Marine Dissolved Organic Matter 2<sup>nd</sup> Ed.,  
22 66-126, 2015.

1 Casciotti, K.L., D.M. Sigman, M. Galanter Hastings, J.K. Böhlke, and A. Hilkert: Measurement  
2 of the oxygen isotopic composition of nitrate in seawater and freshwater using the denitrifier  
3 method. *Anal. Chem.* 74: 4905-4912, 2002.

4 Gerke, L.: pCO<sub>2</sub> in the Mediterranean Sea during the cruise MSM72. Master thesis, Department  
5 of Chemistry, Christian-Albrechts-University Kiel, 2020

6 Clayton, T.D. and Byrne, R.H.: Spectrophotometric seawater pH measurements: total hydrogen  
7 ion concentration scale concentration scale calibration of *m*-cresol purple and at-sea results.  
8 *Deep-sea Res. I*, 40, 10, 2115-2129, 1993.

9 Gonnelli, M., Galletti, Y., Marchetti, E., Mercadante, L., Brogi, S.R., Ribotti, A., Sorgente, R.,  
10 Vestri, S., Santinelli, C.: Dissolved organic matter dynamics in surface waters affected by oil  
11 spill pollution: Results from the serious game exercise, *Deep Sea Res. Part II Top. Stud.*  
12 *Oceanogr.*, 133, 88–99, 2016.

13 Granger, J., and D.M. Sigman. 2009. Removal of nitrite with sulfamic acid for nitrate N and O  
14 isotope analysis with the denitrifier method. *Rapid Commun. Mass Spectrom.* 23: 3753-3762,  
15 doi:10.1002/rcm.4307.

16 Häder, D.-P. and Sinha, R. P.: Solar ultraviolet radiation-induced DNA damage in aquatic  
17 organisms: potential environmental impact. <https://doi.org/10.1016/j.mrfmmm.2004.11.017>,  
18 2005.

19 Hainbucher, D., Álvarez, M., Astray, B., Bachi, G., Cardin, V., Celentano, P., Chaikakis, S.,  
20 Chaves Montero, M. M., Civitarese, G., El Rahman Hassoun, H., Fajar, N. M., Fripiat, F.,  
21 Gerkel, Gogou, A., Guallart, F., Gülk, B., Lange, N., Rochner, A., Santinelli, C., Schroeder,  
22 K., Steinhoff, Tanhua, T., Urbini, L., Velaoras, D., Wolf, F. and Welsch, A.: Variability and  
23 Trends in Physical and Biogeochemical Parameters of the Mediterranean Sea.  
24 <http://epic.awi.de/47567/2/msm71-74-expeditionsheft.pdf>, 2018.

25 Hansell, D.A., Carlson, C.A., Pepeta, D.L. and Schlitzer, R.: Dissolved Organic Matter in the  
26 Ocean: A controversy stimulates new insights. *Oceanog.* 22, 4, 202-211, 2009.

27 Hansen, H. P. & Koroleff e.: Determination of nutrients. In Grasshoff K., K. Kremling & M.  
28 Ehrhardt (eds), *Methods of seawater analysis*. Wiley VCH, Weinheim: 159–228, 1999.

29 Herndl, G.J., Müller-Niklas, G. and Frick, J.: Major role of ultraviolet-B in controlling bacterio  
30 plankton growth in the surface layer of the ocean. *Nature* 361:717-719, 1993.

1 Johnson, K.M., Wills, K.D., Butler, D.B., Johnson, W.K., Wong, C.S., (1993). Coulometric  
2 total carbon dioxide analysis for marine studies: maximizing the performance of an automated  
3 gas extraction system and coulometric detector. *Marine Chemistry*, 44, 167-187.

4 Langdon, C.: Determination of dissolved oxygen in seawater by Winkler titration using the  
5 amperometric technique. IOCCP Report N°14, ICPO publication series N 134, 2010.

6 Li, P., and Tanhua, T.: Medusa-Aqua system: simultaneous measurement and evaluation of  
7 novel potential halogenated transient tracers HCFCs, HFCs and PFCs in the ocean. *Ocean Sci.*  
8 *Discuss.* 2019, 1-34, 2019

9 Li, P., and Tanhua, T.: Recent Changes in Deep Ventilation of the Mediterranean Sea; Evidence  
10 from Long-Term Transient Tracer Observations. *Frontiers in Marine Science*  
11 7.10.3389/fmars.2020.00594, 2020

12 Malanotte-Rizzoli, P., Artale, V., Borzelli-Eusebi, G. L., Brenner, S., Civitarese, G., Crise, A.,  
13 Font, J., Gacic, M., Kress, N., Marullo, S., Ozsoy, E., Ribera d'Alcalà, M., Roether,  
14 W., Schroeder, K., Sofianos, S., Tanhua, T., Theocharis, A., Alvarez, M., Ashkenazy,  
15 Y., Bergamasco, A., Cardin, V., Carniel, S., D'Ortenzio, F., Garcia-Ladona, E., Garcia-  
16 Lafuente, J. M., Gogou, A., Gregoire, M., Hainbucher, D., Kontoyannis, H., Kovacevic, V.,  
17 Krasakapoulou, E., Krokos, G., Incarbona, A., Mazzocchi, M. G., Orlic, M., Pascual, A.,  
18 Poulain, P.-M., Rubino, A., Siokou-Frangou, J., Souvermezoglou, E., Sprovieri, M., Taupier-  
19 Letage, I., Tintoré, J., and Triantafyllou, G.: Physical forcing and physical/biochemical  
20 variability of the Mediterranean Sea: a review of unresolved issues and directions for future  
21 research. *Ocean Science* Vol.10, Issue 3, 281-322, 2014

22 Margolin, A.R., Gonnelli, M., Hansel, D.A. and Santinelli, C.: Black Sea dissolved organic  
23 matter dynamics: Insights from optical analyses. *Limnol. Oceanogr.* 63, 3, 1425-1443, doi:  
24 10.1002/lno.10791, 2018.

25 Mintrop, L., Pérez, F. F., González-Dávila, M., Körtzinger, A. and Santana-Casiano, J.M.:  
26 Alkalinity determination by potentiometry-intercalibration using three different methods.  
27 *Ciencias Marinas*, 26, 1, 23-37., 2000.

28 Nelson, N.B. and Siegel, D.A.: The global distribution and dynamics of chromophoric dissolved  
29 organic matter. *Annu. Rev. Mar. Sci.*, 5, 447-476, 2013.

30 Patsavas, M.C., Byrne, R.B., Yang, B., Easley, R.A., Wanninkhof, R., Liu, X.: Procedures for  
31 direct spectrophotometric determination of carbonate ion concentrations: Measurements in US  
32 Gulf of Mexico and East Coast waters. *Mar. Chem.*, 168, 80-85, 2015.



1 Pérez, F.F. and Fraga F.: A precise and rapid analytical procedure for alkalinity determination.  
2 Marine Chemistry, 21, 169-182, 1987.

3 Pérez, F.F., Ríos, A.F., Rellán, T. and Álvarez, M.: Improvements in a fast potentiometric  
4 seawater alkalinity determination. Ciencias Marinas, 26, 463-478, 2000.

5 Retelletti Brogi, S. Gonelli, M., Vestri, S. and Santinelli, C.: Biophysical processes affecting  
6 DOM dynamics at the Arno river mouth (Tyrrhenian Sea). Biophysical Chemistry, 197, 1-9,  
7 2015.

8 Roether, W., Klein, B., and Hainbucher, D.: The Eastern Mediterranean Transient: Evidence  
9 for Similar Events Previously? In: The Mediterranean Sea: Temporal Variability and Spatial  
10 Patterns, edited by: Borzelli, G. L. E., AGU monographs, 2013

11 Santinelli, C., Follet C., Retelletti Brogi, S., Xu, L., Repeta, D.: Carbon isotope measurements  
12 reveal unexpected cycling of dissolved organic matter in the deep Mediterranean Sea. Mar  
13 Chem., 177, 267-277, 2015.

14 Santinelli, C.: DOC in the Mediterranean Sea. In: Biogeochemistry of Marine Dissolved  
15 Organic Matter 2<sup>nd</sup> Ed., 579-608, 2015.

16 Santinelli, C., Hansell, D. A. and Ribera d'Alcala, M.: Influence of stratification on marine  
17 dissolved organic carbon (DOC) dynamics: The Mediterranean Sea case. Prog. Oceanogr., 119,  
18 68-77, 2013.

19 Santinelli, C., Nannicini, L. and Seritti, A. : DOC dynamics in the meso and bathypelagic layers  
20 of the Mediterranean Sea. Deep-Sea Res. II, 57, 1446-1459, 2010.

21 Schneider, A., Tanhua, T., Körtzinger, A., and Wallace, D. W. R.: High anthropogenic carbon  
22 content in the eastern Mediterranean, J. Geophys. Res., 115, C12050, doi:  
23 10.1029/2010JC006171, 2010.

24 Schroeder, K., Gasparini, G. P., Tangherlini, M. and Astraldi, M.: Deep and intermediate water  
25 in the western Mediterranean under the influence of the Eastern Mediterranean Transient.  
26 Geophys. Res. Lett., doi: 10.1029/2006GL027121, 2006.

27 Schroeder, K., Ribotti, A., Borghini, M., Sorgente, R., Perilli, A., and Gasparini, G. P.: An  
28 extensive western Mediterranean deep water renewal between 2004 and 2006, Geophys. Res.  
29 Letters, 35, 2008.

30 Stedmon, C.A. and Nelson, N.B.: The optical properties of DOM in the Ocean. In:  
31 Biogeochemistry of Marine Dissolved Organic Matter 2<sup>nd</sup> Ed., 481-508, 2015.

- 1 Sigman, D.M., K.L. Casciotti, M. Andreani, C. Barford, M. Galanter, and J.K. Böhlke: A  
2 bacterial method for the nitrogen isotopic analysis of nitrate in seawater and freshwater. *Anal.*  
3 *Chem.* 73: 4145-4153, 2001.
- 4 Tanhua, T., Hainbucher, D., Schroeder, K., Cardin, V., Álvarez, M., and Civitarese, G.: The  
5 Mediterranean Sea system: a review and an introduction to the special issue, *Ocean Sci.*, 9, 789-  
6 803, doi:10.5194/os-9-789-2013.
- 7 Turnherr, A.M.: How to Process LADCP Data with the LDEO Software (Versions IX.7 –  
8 IX.10). The “go-ship” manual for LADCP data acquisition ftp:  
9 [//ftp.ldeo.columbia.edu/pub/LADCP/UserManuals](ftp://ftp.ldeo.columbia.edu/pub/LADCP/UserManuals), 2014.
- 10 Ullmann, D. S. and Hebert, D.: Processing of Underway CTD data. AMS  
11 <https://doi.org/10.1175/JTECH-D-13-00200.1>, 2014.
- 12 Weigand, M.A., J. Foriel, B. Barnett, S. Oleynik, and Sigman, D. M.: Updates to  
13 instrumentation and protocols for isotopic analysis of nitrate by the denitrifier method. *Rapid*  
14 *Commun. Mass Spectrom.* 30: 1365-1383, 2016.